



Su, H., Psyrras, N., Crispin, J. J., Karamitros, D. K., & Mylonakis, G. (2019). *Transmission Of Foundation Vibrations*. Paper presented at Society for Earthquake and Civil Engineering Dynamics Conference, London, United Kingdom.

Peer reviewed version

License (if available):
CC BY-NC

[Link to publication record in Explore Bristol Research](#)
PDF-document

University of Bristol - Explore Bristol Research

General rights

This document is made available in accordance with publisher policies. Please cite only the published version using the reference above. Full terms of use are available:
<http://www.bristol.ac.uk/pure/about/ebr-terms>

TRANSMISSION OF FOUNDATION VIBRATIONS

Huize SU¹, Nikolaos PSYRRAS², Jamie CRISPIN², Dimitris KARAMITROS³ & George MYLONAKIS⁴

Abstract: *Ground vibrations triggered by machine foundations can influence adjacent structures in both serviceability and durability limit states. In order to control the potential damage to structures in the vicinity of the source, it is important to be able to predict the response of the surrounding soil. This study investigates the soil response induced by a harmonically loaded foundation with coupled swaying-rocking motion embedded in a soil layer over a half-space with the use of finite-element models developed in Abaqus. The soil medium is modelled in the frequency-domain as a linearly elastic material with frequency-independent damping. Appropriate 'non-reflective' conditions are applied at the boundaries to minimise wave reflections. Initially, an axisymmetric model of homogeneous half-space is developed, with anti-symmetric boundary conditions applied to simulate coupled swaying-rocking oscillations. To establish a general trend for the spatial attenuation of vibration amplitude, multi-variable functions are fitted to the results obtained from these analyses. The proposed relations are subsequently employed for a preliminary assessment of the vibrations transmitted by the shaking table and reaction mass of the new University of Bristol Soil Foundation Soil Structure Interaction Facility (SoFSI). Noting that the final configuration of the facility is still under design and that the soil properties have not been accurately established yet, this case study allows for useful comparisons between analytical solutions and a full three-dimensional finite-element simulation.*

1. Introduction

One of the elementary goals in the design of foundations subjected to machine-type loadings, is to limit their motion amplitudes to within certain thresholds, so that machine foundation vibrations will not disturb the adjacent environment, such as neighbouring structures (Gazetas, 1983). The dynamic response of machine foundations has been analysed using the simplified Mass-Spring Dashpot (MSD) or Winkler model (Hetenyi, 1946, Terzaghi, 1955, Barkan, 1962 and Prakash and Puri, 2006), a small elastic half-space (Lamb, 1904, Reissner, 1936, Sung, 1953, Gong et al. 2006 and Chowdhury and Dasgupta 2008), reduced domain using Lysmer boundary elements (Lysmer, 1965). Gazetas (1991a, 1991b) presented a range of simplified formulas and design charts for the soil-structure stiffness at a particular frequency under different vibration modes, for both surface and embedded machine foundations with different shapes. The above analysis generally concentrates on the dynamic response of the soil near the sources of ground vibration. This allows engineers to control the effects of machine foundation vibrations in design.

However, for some machine-type loaded foundations (such as shaking tables), large amplitude vibrations are inherent. In order to avoid the large amplitude ground vibration causing structural damage to existing buildings in the vicinity of the source, the study of vibration propagation and attenuation through the soil domain to the far-field is required.

Due to the complexity of the problem, related mainly to the inhomogeneity of the soil and modelling the soil boundary conditions, realistically, wave attenuation in soil media is often analysed numerically. Finite element (FE) simulations of wave propagation and attenuation were mostly carried out for common ground vibration sources, such as hammer compaction, pile driving, blasting and transport loading (Yang and Huang, 1997, Hall, 2003 and Yang et al., 2003). Nevertheless, the input motions were mostly taken from field test recordings. This means that the

¹ Undergraduate Student, University of Bristol, United Kingdom

² PhD Student, University of Bristol, United Kingdom

³ Lecturer in Geotechnical Engineering, University of Bristol, United Kingdom

⁴ Chair in Geotechnics and Soil-Structure Interaction, University of Bristol, United Kingdom, g.mylonakis@bristol.ac.uk

solutions are strongly case-dependent and are not reliable to generalise to the case of machine foundations.

In this paper, the FE software Abaqus is employed to develop numerical models of wave propagation induced by the harmonic forced vibration of a rigid shallow foundation. The characteristics of the wave attenuation from the source are studied using a 2-D axisymmetric model, where the soil is modelled as a homogeneous half-space. The simulations are run using the 'direct-steady-state dynamic' analysis procedure formulated in the frequency domain. Two excitation modes are considered, namely swaying and rocking, and an attenuation relationship is developed by adopting the dynamic stiffness of the foundation (Mylonakis et al., 2006) and a wave attenuation equation.

In view of the above, a preliminary assessment of the vibrations generated by the new University of Bristol Soil Foundation Structure Interaction (SoFSI) Facility is performed. This facility will include a large shaking table attached to a rectangular reaction mass to be fully embedded in a bi-layered soil deposit. The dynamic response of the foundation due to shaking table operation is initially evaluated analytically, and the vibrations transmitted to neighbouring structures are estimated with the aid of the proposed attenuation relationship. The obtained results are then compared against the predictions of a full 3-D finite element model, run on University of Bristol's HPC BlueCrystal 3. It is emphasized that the design of the Bristol SoFSI Facility is still ongoing, hence this analysis is performed for a concept configuration that might differ from the final one. Furthermore, as the geotechnical investigation had not been completed at the time of the analysis, this work is based on preliminary estimations of the associated soil parameters and the results obtained herein might not be compatible with the performance to be specified by the final design.

2. Wave propagation in homogeneous half-space

2.1 Wave propagation

The propagation of ground vibrations depends on the type of excitation source, frequency of vibration, distance between the source and the receiver and geometry. Vibrations are transmitted through the soil media by body waves (P-wave and S-wave) and surface waves (mainly Rayleigh waves) (Kramer 1996; Massarsch 2000). Figure 1 illustrates the wave propagation in a half-space caused by a ground vibration on the soil surface. Body waves propagate through the soil with hemispherical wave fronts, while Rayleigh waves propagate radially outward along the surface.

Equations (1) and (2) represent the attenuation functions of body waves and Rayleigh waves, respectively, along the surface of elastic half-space (Braja and Ramana, 2011). It shows that the amplitude of Rayleigh waves attenuates slower than body waves with distance from the source, r . This means Rayleigh waves can cause larger ground displacement than body waves at distance r , when the same vibration amplitude is applied at the excitation source. Therefore, Rayleigh waves are identified as the most critical wave form in this study.

$$\text{Amplitude} \propto \frac{1}{r} \quad (3\text{-D Body wave}) \quad (1)$$

$$\text{Amplitude} \propto \sqrt{\frac{1}{r}} \quad (3\text{-D Rayleigh wave}) \quad (2)$$

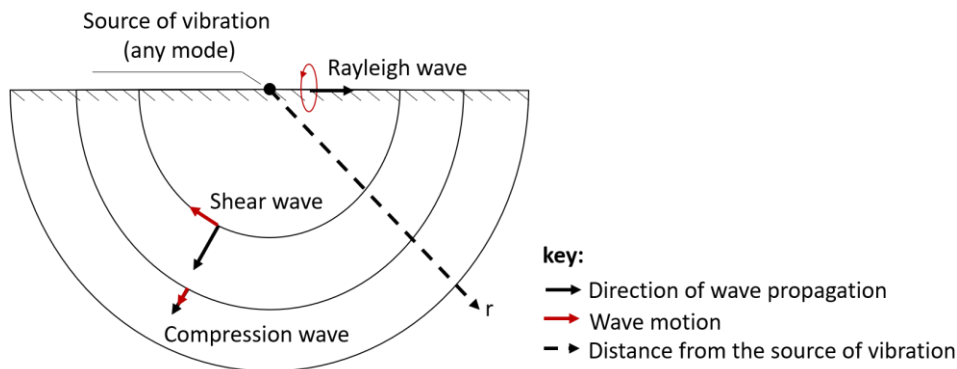


Figure 1: Propagation of body waves and Rayleigh waves in elastic half-space

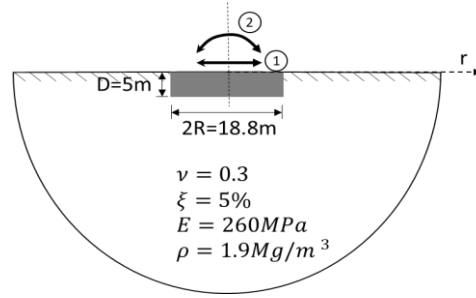


Figure 2: Model of circular foundation embedded in homogeneous half-space: (1) horizontal swaying vibration and (2) rocking vibration

2.2 Development of the finite element model

In this section, a 2-D numerical model is developed for analysing the wave attenuation in an elastic half-space from a harmonically excited embedded shallow foundation. The dimensions of the foundation and the material properties are shown in Figure 2. A hysteretic damping ratio $\xi = 5\%$ was adopted for the soil domain. Horizontal swaying and rocking oscillations are applied harmonically to the foundation with a frequency range of 0 – 50Hz. Wave attenuation is analysed along the soil surface in the radial longitudinal direction (along r).

The FE code Abaqus was employed in this study. To account for three-dimensional attenuation effects in a computationally efficient way, an axisymmetric model is opted. The model consists of a circular foundation with radius, $R = 9.4m$, and depth, $D = 5m$ embedded in a soil domain, which has dimensions $width \times depth = 30R \times 50D$ ($282m \times 250m$). The circular foundation is assumed to be fully rigid and the footing surfaces are assumed rough. Therefore, the foundation is simulated by constraining the nodes at the interface between the foundation and soil in all degrees of freedom. Harmonic vibrations of the foundation are defined as a harmonic displacement to a master node on the interface. As a result, the model is simplified in that only the soil body is needed to be modelled, and it reduced the computational cost.

The finite elastic soil domain is modelled using four-node bilinear axisymmetric elements with reduced integration and hourglass control (CAX4R). In order to avoid filtering of high wave frequencies by large elements, Kuhlemeyer and Lysmer (1973) suggest a relationship between the maximum element size and shortest wavelength:

$$L_{max} \leq \frac{1}{8} \lambda_{min} \quad (3)$$

In this study, the maximum element size, L_{max} was determined based on the minimum Rayleigh wavelength, $\lambda_{R,min}$, which can be calculated using equation (4) by applying the highest vibration frequency of interest, f_{max} .

$$\lambda_{R,min} = \frac{V_R}{f_{max}} \quad (4)$$

where the velocity of Rayleigh wave, V_R , can be determined from equation 5 (Kramer, 1996):

$$V^6 - 8V^4 - (16\alpha^2 - 24)V^2 - 16(1 - \alpha^2) = 0 \quad (5)$$

In which $V = V_R/V_s$. The shear wave velocity, V_s , can be calculated through the relationship between shear modulus of soil (G) and soil density (ρ).

$$V_s = \sqrt{\frac{G}{\rho}} = \sqrt{\frac{E}{2(1+\nu)\rho}} \quad (6)$$

Braja and Ramana (2011) proposed an equation expressing α in terms of Poisson's ratio, ν :

$$\alpha = \sqrt{\frac{1-2\nu}{2-2\nu}} \quad (7)$$

A maximum excitation frequency of 50Hz was employed to the model. By substituting equation (6) and (7) into equation (5), it can be obtained that $V = 0.93$, and $V_s = 230$ m/s, therefore, the minimum Rayleigh wavelength is calculated as $\lambda_{R,min} = 215$ m/s. According to equation (3), the allowable maximum element size is 0.54m. As a result, the model was discretised into uniform elements with a side length of 0.5m.

2.3 Boundary conditions

An appropriate anti-axisymmetric boundary condition is enforced along the axis of symmetry of the model by restraining the vertical motion of its nodes. Zero-stress conditions are imposed at ground surface. In physical reality, lateral and downward transmission of waves in the ground is unobstructed by physical boundaries and theoretically continues to infinity. Nevertheless, the FE method can only simulate a finite domain. In order to avoid spurious wave reflections at the boundaries of the FE mesh, two methods are considered: a) increasing the distance of the boundaries from the excitation source until the change in attenuation of peak displacement at the ground surface is sufficiently small; b) implement ‘non-reflective’ boundaries to replace the far-field region. The first method relies on geometrical damping to achieve its goal. The energy is expected to be entirely dissipated when the size of the model is big enough. However, it can be time-consuming and computationally intensive. Therefore, ‘non-reflective’ boundaries are applied at the bottom and lateral boundaries of the model.

Absorbing-boundaries model have been implemented in Abaqus by means of special ‘infinite elements’ that can be used as a ‘non-reflective’ boundary (Abaqus, 2013). As the model is built under axisymmetric condition and the finite solid part was modelled as four-node bilinear elements, for consistency, the ‘non-reflective’ boundaries are modelled as four-node, axisymmetric, continuum infinite elements (CINAX4). The geometry of the model is shown in Figure 3(a) and the mesh layout is shown in Figure 3(b). A region of 20R from source along the surface is of interest in this study. Therefore, a 10R-thick layer surrounding the near-field region is replaced by ‘infinite elements’.

To verify the effectiveness of this approach, a comparison was drawn against the response of a model with a fixed far-field boundary (the bottom boundary remaining ‘non-reflective’). In addition, a smaller dimensioned model was created to compare against, also with a fixed boundary.

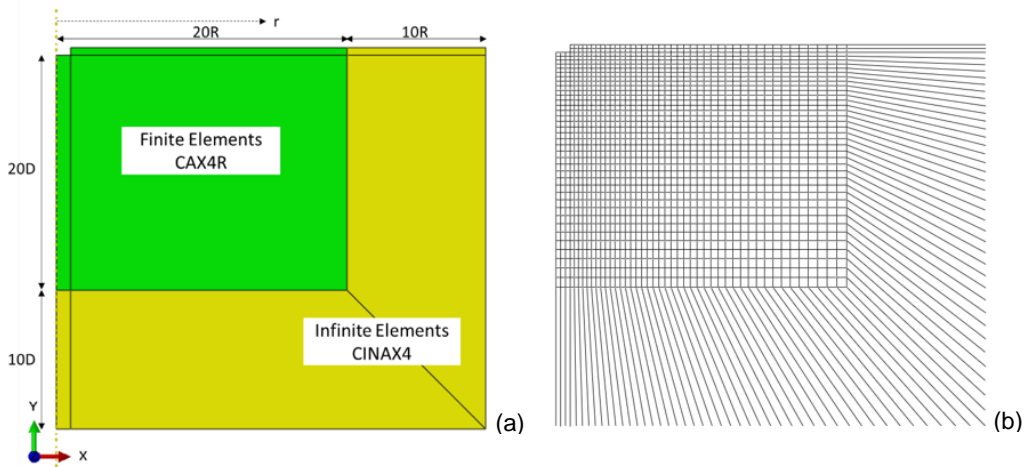


Figure 3: (a) Dimensions and (b) the mesh layout of the dynamic finite element model of ground vibration propagation in Abaqus featuring a near-field region comprising conventional finite elements and a far-field region comprising infinite elements

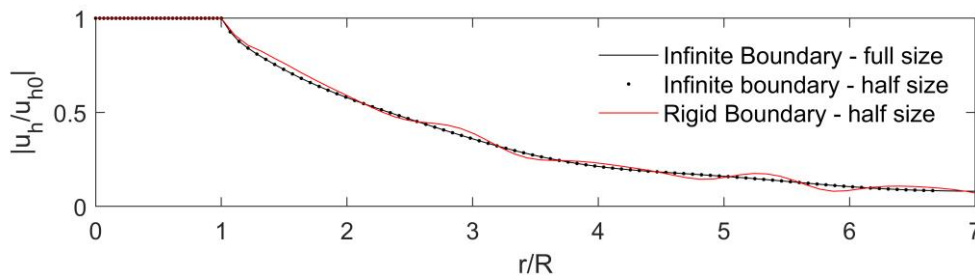


Figure 4: Circular rigid footing on half-space: attenuation of horizontal displacement with horizontal distance from the footing in horizontal vibration mode with different boundary conditions

Ground vibration is generated by horizontal swaying of the rigid foundation at a frequency of $\omega = 110 \text{ rad/s}$, which is then normalised, so its absolute value is arbitrary. The amplitude of the normalised horizontal displacement ($|u_h/u_{h0}|$), where u_{h0} is the maximum footing horizontal displacement, is plotted against the normalised horizontal distance (r/R) from the excitation source along the free surface of the soil in Figure (4).

It is seen that, in the smaller geometries, the model with ‘non-reflective’ boundary produced results identical to the extended geometry models, while the one with a fixed far-field boundary gave a rather noisy curve, as expected. The results demonstrate that wave reflection will not affect the wave attenuation profile in a model with a ‘non-reflective’ boundary, because at least a great part of the vibration energy is absorbed by the infinite elements.

2.4 Wave attenuation due to foundation vibrations

Figure (5) shows the profiles of wave attenuation due to horizontal swaying and rocking foundation vibrations for different excitation frequencies. The forcing frequencies are represented in a dimensionless form of $\omega R/V_R$ (i.e., $\omega R/V_R = 0, 1, 3, 6, 9, 12$). Attenuation profiles are calculated along a surface path $r/R = 20$ ($r = 188\text{m}$) from the centre of the footing. From $r/R = 0$ to 1, the constant $|u_h/u_{h0}|$ (Figure (5a)) and the linear variation of $|u_v/u_{v0}|$ (Figure (5b)) reveal the perfect rigidity of the foundation. The value u_{v0} represents the maximum vertical displacement of the rigid foundation under the harmonic motion. There is a significant variation in the amplitude of displacement from $r/R = 1$ to 5 ($r = 9.4\text{m} - 47\text{m}$). The attenuation of displacement is sharpest for the static case ($\omega R/V_R = 0$). For the dynamic cases, attenuation curves are approaching zero in a wavy pattern as distance increases.

The vibration with high frequencies generates larger soil surface displacement than those with lower frequencies near the source ($1 < r/R < 5$). In contrast, soil displacements are smaller for high excitation frequencies than those for low excitation frequencies, as the distance from the ground vibration increases (i.e. $r/R = 20$).

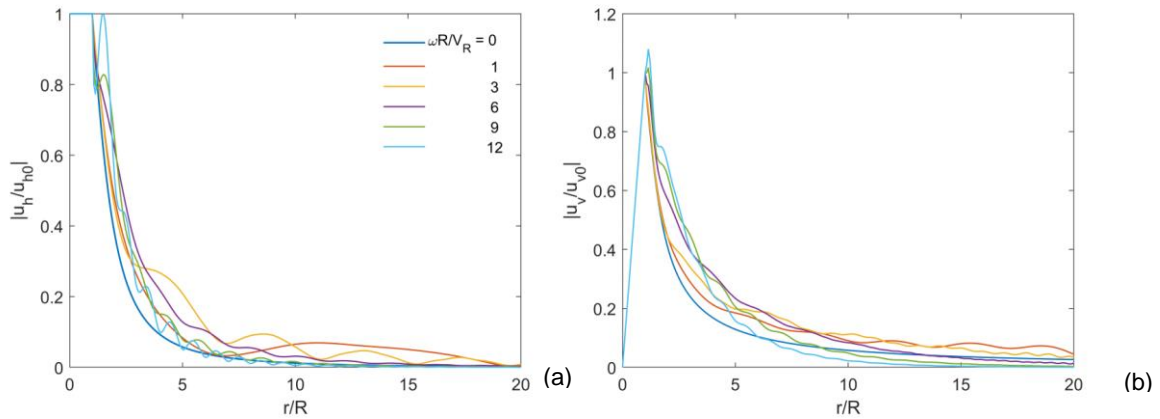


Figure 5: Circular rigid footing on half-space: attenuation of (a) horizontal displacement and (b) vertical displacement with horizontal distance from the footing in horizontal vibration mode; $\nu = 0.3, \xi = 5\%$

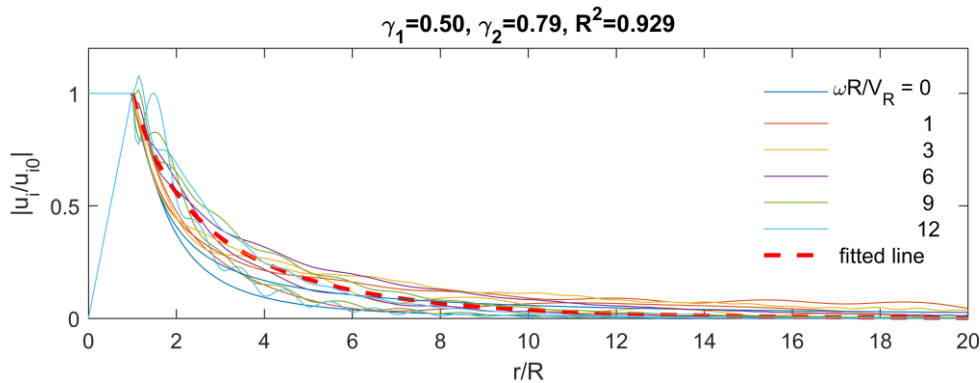


Figure 6: Curve-fitting of the displacement attenuation profiles in half-space

At the same distance from the source, the amplitudes of the vertical displacements due to foundation rocking are larger than those of the horizontal displacement due to foundation swaying. This indicates that the ground vibration in a rocking mode has potentially more pronounced effect to nearby structures.

2.5 Characterisation of wave attenuation half-space

The attenuation properties of ground vibration are dependent on the type of vibration excitation. Attenuation of the vibration amplitudes during propagation through the soil is mainly caused by geometrical damping and soil material damping. The purpose is to investigate the attenuation properties of two ground vibration modes (horizontal swaying and rocking) for different frequencies.

Bornitz (1931) proposed an expression that describes the attenuation of the amplitude of ground vibration with distance from the excitation source:

$$\left| \frac{u_i}{u_{i0}} \right| = \left(\frac{R}{r} \right)^{\gamma_1} e^{-\alpha \left(\frac{r-R}{R} \right)} \quad (8)$$

in which u_{i0} represents the maximum displacement amplitude in either horizontal (swaying) or vertical (rocking) directions, of the vibrating rigid foundation. The amplitude of the transmitted vibration along the soil surface is represented by u_i ; γ_1 is a geometric damping factor and α is a material damping factor. In order to analyse the influence of excitation frequency on the displacement attenuation, the material damping coefficient was expressed in a dimensionless form as:

$$\alpha = \gamma_2 \xi \left(\frac{\omega R}{V_R} \right) \quad (9)$$

where γ_2 is the loss factor of the attenuation.

As the Rayleigh waves are treated to be the critical propagation form, the factor γ_1 is taken as 0.5. The numerically evaluated attenuations functions for both horizontal and rocking vibration, were fitted to equation (8), using least square. As shown in Figure 6, the factor γ_2 is determined as 0.8. The goodness of the fits is demonstrated by the coefficient of determination R^2 , which is close to one.

3. The Bristol SoFSI Facility case study

In this section, a case study is presented, where the problem is extended to a harmonically vibrating rigid rectangular foundation, fully embedded in a soft soil layer over stiffer bedrock. The geometrical characteristics of the foundation and the applied excitation correspond to a possible concept configuration of the new University of Bristol Soil-Foundation-Structure Interaction (SoFSI) Facility, which is currently under design. The configuration analysed herein includes a 50t capacity shaking table and a soil pit, built in a concrete reaction mass with a total mass $m = 2454t$ and external dimensions $2B \times 2L \times D = 11m \times 25m \times 5m$, as shown in Figure 7. The shaking table, including the platform, specimen and ancillaries, has a total moving mass of $m_m = 85t$, its centre of gravity is assumed to be at the surface of the foundation, while its motion is taken as horizontal and harmonic, with an acceleration amplitude $a_m = 1.52g$ ($g = 9.81m/s^2$) for a frequency range $f = 3 - 20Hz$. The foundation is assumed to be fully embedded in a 5m deep clay layer with shear modulus $G = 100MPa$, Poisson's ratio $\nu = 0.3$ and density $\rho = 1.9Mg/m^3$, underlain by mudstone with $G = 100MPa$, $\nu = 0.4$ and $\rho = 2.2Mg/m^3$. Material damping was taken as $\xi = 5\%$. Note that the aforementioned soil properties are preliminary estimations of the actual in-situ conditions, as the results from a detailed geotechnical investigation were not available at the time of the analysis.

3.1 Analytical solution

The dynamic response of the foundation, namely the base horizontal displacement u_y and the rotation θ_x , were initially obtained analytically ignoring torsional effects ($\theta_z = 0$) as follows:

$$\begin{Bmatrix} u_{y,0} \\ \theta_{x,0} \end{Bmatrix} = \left(\begin{bmatrix} \bar{K}_y & \bar{K}_{y,rx} \\ \bar{K}_{y,rx} & \bar{K}_{rx} \end{bmatrix} + i\omega \begin{bmatrix} C_y & C_{y,rx} \\ C_{y,rx} & C_{rx} \end{bmatrix} - \omega^2 \begin{bmatrix} m & m \frac{D}{2} \\ m \frac{D}{2} & I_o \end{bmatrix} \right)^{-1} \begin{Bmatrix} m_m a_m \\ m_m a_m D \end{Bmatrix} \quad (10)$$

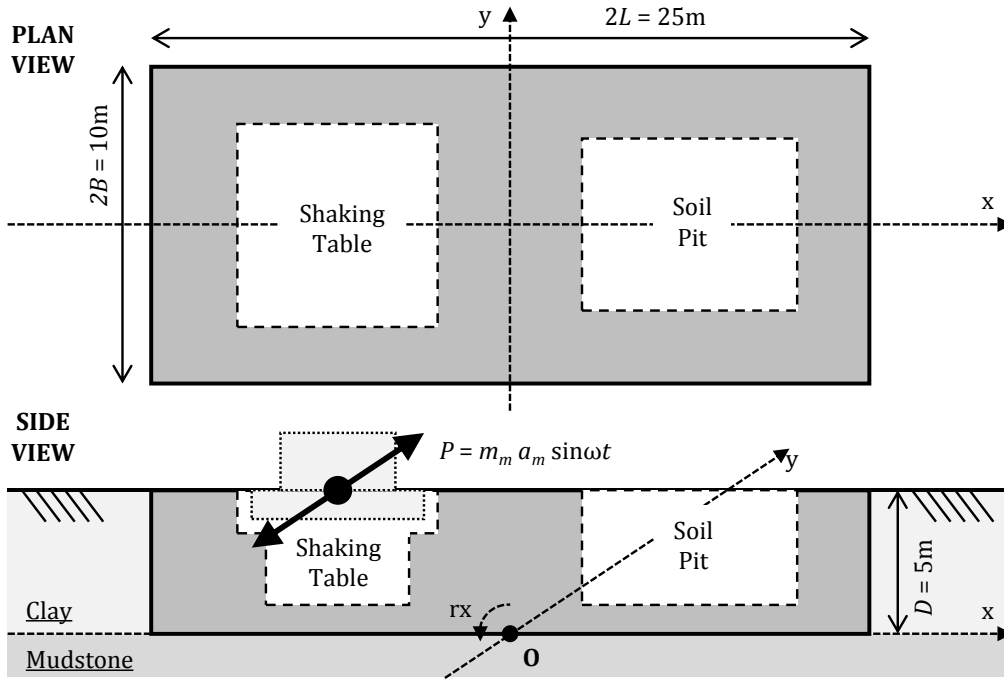


Figure 7: Analyzed configuration of the Bristol SoFSI Facility

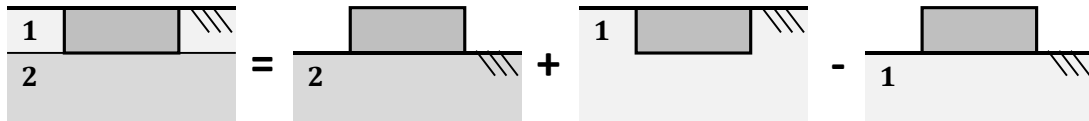


Figure 8: Superposition assumed for the bi-layered soil deposit

where \bar{K}_y , \bar{K}_{rx} and $\bar{K}_{y,rx}$ are the lateral horizontal, rocking and swaying-rocking coupling term of the frequency-dependent dynamic stiffness, C_y , C_{rx} and $C_{y,rx}$ are the corresponding dashpot coefficients, $\omega = 2\pi f$ is the angular frequency and I_o is the mass moment of inertia of the foundation about the base longitudinal axis x .

It is reminded that no analytical expressions of the above dynamic stiffnesses and dashpot coefficients are available for bi-layered soil deposits like the one examined herein. Therefore, these terms were estimated assuming the superposition that is schematically illustrated in Figure 8. For example, the horizontal stiffness was calculated as:

$$\bar{K}_y = \bar{K}_y^{surf,2} + \bar{K}_y^{emb,1} - \bar{K}_y^{surf,1} \quad (11)$$

where the superscripts *surf, 2*, *emb, 1* and *surf, 1* imply “at the surface of layer 2”, “embedded in layer 1” and “at the surface of layer 1”, respectively. The corresponding quantities for surface and embedded foundations were calculated according to Gazetas (1991a, 1991b). Furthermore, it is noted that material damping was taken into account in the dashpot coefficients as follows:

$$C^{total} = C^{radiation} + \frac{2\bar{K}\xi}{\omega} \quad (12)$$

Finally, the total displacement of the foundation at the surface was calculated as:

$$u_{y,t} = u_{y,o} + \theta_{x,o} \cdot D \quad (13)$$

This was then attenuated using Equations (8) and (9), to derive the transmitted vibrations in the form of horizontal displacement, velocity and acceleration, at different distances from the facility. Since the critical transmitted waves are Rayleigh (surface) waves, the soil parameters corresponding to the top clay layer were used in the calculations.

3.2 3-D numerical model

The plan of the meshed 3-D model is shown in Figure 8 along with its dimensions. The elastic soil domain is modelled with linear eight-node brick elements with reduced integration (C3D8R).

3-D infinite elements (CIN3D8) are employed to act as ‘non-reflective’ boundaries. A steady-state dynamic analysis is undertaken in the frequency-domain. Based on the Rayleigh wave velocity in the topsoil layer ($V_{R1} = 215\text{m/s}$) and the relationship between wavelength and element size of the model (equation 3), a mesh with a uniform element size of 1m was generated.

In order to capture the influence of the slab embedment, the vibrating slab is simulated explicitly in the numerical model as a rigid body with perfectly rough surfaces (no slip between slab and soil). Due to the effect of the embedment and roughness of the slab, as well as the eccentricity between the applied force and the resultant resistant forces, the obtained movement of the slab is coupled horizontal swaying and rocking.

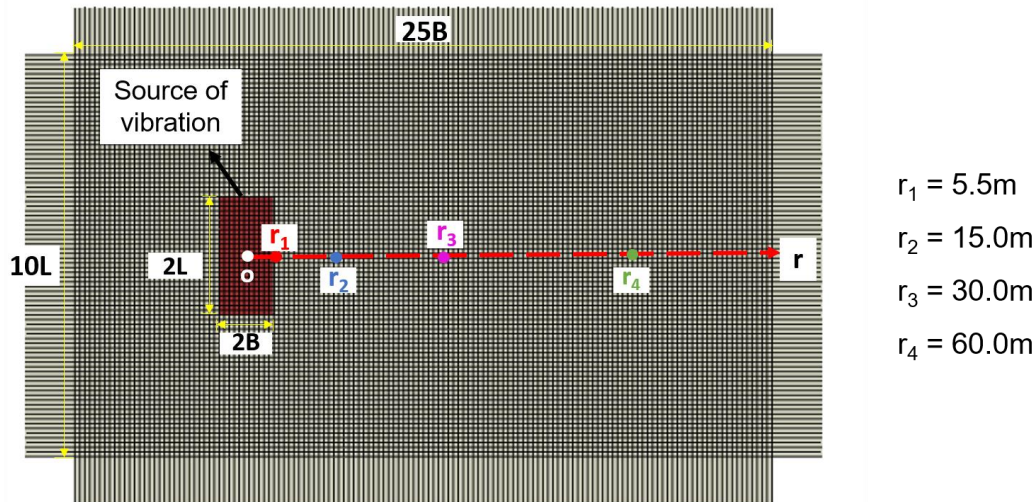


Figure 9: Plan view of undeformed mesh with model dimensions

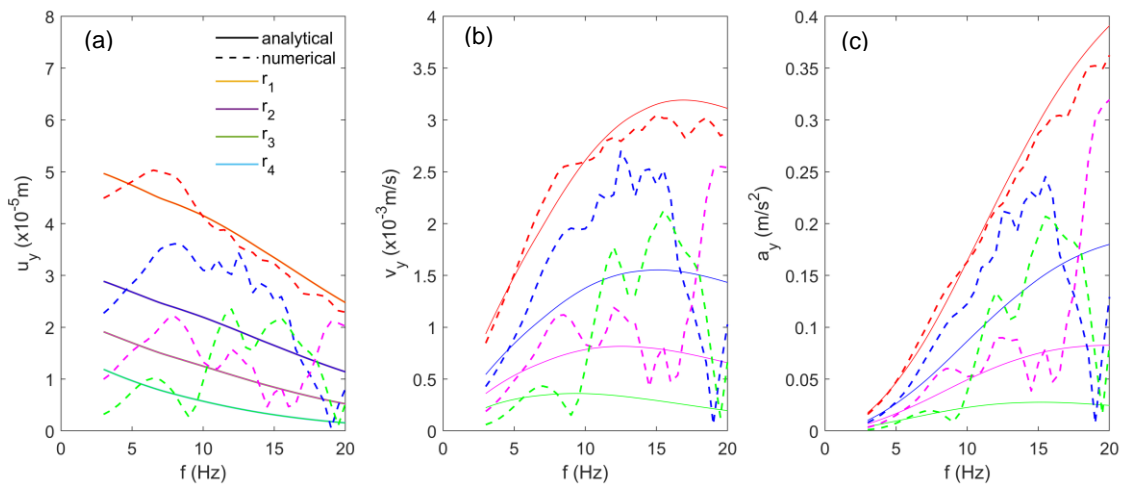


Figure 10: Predicted horizontal (a) displacement (b) velocity (c) acceleration against frequencies

3.3 Comparison against analytical formulae

To gauge the reliability of both the analytical solution and the numerical analysis for this case study, the results obtained from the 3-D model are compared with the analytical results. As shown in Figure 9, four stations on the soil surface are chosen along the longitudinal direction from the source. The responses of the soil surface are compared against the analytical solutions for the examined frequency range in Figure 10, in terms of the variation of the absolute amplitudes of horizontal displacement $|u_y|$, velocity $|v_y|$ and acceleration $|a_y|$ with the applied excitation frequency.

A good agreement can be observed between the analytically and numerically obtained results, especially for small excitation frequencies and for stations close to the excitation source. This

indicates that the assumed superposition used for the analytical calculations provides good predictions of the dynamic response of the foundation. Nevertheless, discrepancies are obtained for further stations and high-frequency excitations. This is likely due to wave reflections between the interface layer and the soil surface, which are not taken into account by the attenuation relationship. The far-field boundary might also contribute to wave reflection, especially in the presence of a bi-layered soil deposit. Still, it is demonstrated that the proposed attenuation relationship provides reasonably accurate predictions, at least for preliminary design purposes.

4. Conclusions and recommendations for further work

In this study, a numerical investigation of the wave attenuation produced by a harmonically vibrating source in different vibration modes was conducted in the frequency-domain using the FE software Abaqus. Simulations were carried out based on the assumption of a linear-elastic soil material. Based on the results presented, the following conclusions were drawn:

- Numerical results are compared well against the analytical solution for close distances and low excitation frequencies.
- An infinite soil domain can be numerically approximated by introducing special infinite elements to enforce a 'non-reflective' boundary condition; rigid boundary conditions were shown to cause unrealistic wave reflections, even if the boundaries are located at large distances from source.
- The effect of the high frequency foundation vibration is more pronounced than that of the lower frequencies for the soil in vicinity of the ground vibration.
- Waves generated from lateral oscillations of the foundation attenuate faster than those from rocking oscillations in half-space.

Further development based on this study could include investigating the influence of:

- Wave attenuation in the transverse direction from the ground vibration source.
- Wave propagation in a layer over rigid bedrock.
- Different shapes of foundation as the vibration source using 3-D numerical simulations.
- Non-linear constitutive laws for the soil material.
- Wave barriers to mitigate the damage to the surrounding structures caused by excessively transmitted vibrations.

REFERENCES

- Abaqus (2013). Abaqus Analysis User Manual – Abaqus Version 6.8. Available at: <http://dsk.ippt.pan.pl/docs/abaqus/v6.13/index.html> (Accessed 30/05/2019)
- Barkan DD (1962), *Dynamics of Bases and Foundations*. New York: McGraw-Hill Book Co., Inc.: 434
- Braja MD and Ramana GV (2011), *Principles of Soil Dynamics*, 2nd Ed, USA Boston: PWS-KENT
- Bornitz, G. (1931). *Über die Ausbreitung der von Groszkolbenmaschinen erzeugten Bodenschwingungen in die Tiefe*, Springer, Berlin (in German).
- Chowdhury I and Dasgupta SP (2008), *Dynamics of Structures and Foundations - a unified approach* Volume 1 and 2 CRC Press, Leiden, Holland
- Gazetas G (1983) Analysis of machine foundation vibrations: State of the art. *Soil dynamics and earthquake engineering*, 2(1): 2-42.
- Gazetas G (1991a), *Foundation vibration*, Foundation Engineering Handbook, Van Nostrand Reinhold, 2nd Ed, 553-593
- Gazetas G (1991b), Formulas and Charts for impedance of surface and embedded foundations. *Journal of Geotechnical Engineering*, 117(9):1370-1381
- Gong SW, Hu LQ and Li XB (2006), Simulation on dynamic response of crack subjected to impact loading. *Explosion and Shock Waves*. *School of Resources and Safety Engineering, Central South University*
- Hall L (2003), Simulation and Analysis of Train-Induced Ground Vibration in Finite Element Models. *Soil Dynamics and Earthquake Engineering*, (23): 403-413

- Hetenyi M (1946), Beams on Elastic Foundation. *The University of Michigan Press* (Ann Arbor). 255
- Kramer SL (1996), Geotechnical earthquake engineering. *Prentice-Hall, Englewood Cliffs*
- Kuhlemeyer RL and Lysmer J (1973), Finite Element Method Accuracy for Wave Propagation Problems. *Journal of the Soil Mechanics and Foundations Division, ASCE*, 99(5): 421-427
- Lamb H (1904), On the propagation of tremors over the surface of an elastic solid. *Philosophical Transactions of the Royal Society of London*, A203,1-42
- Lysmer J (1965), *Vertical Motion of Rigid Footings*, Department of Civil Engineering, University Of Michigan Report to WES Contract Report, N. 3-115 under Contract N. DA-22-079-eng-340
- Mylonakis G, Nikolaou S and Gazetas G (2006), *Footings under seismic loading: Analysis and design issues with emphasis on bridge foundations*. *Soil Dynamics and Earthquake Engineering*, 26: 824–853
- Massarsch KR (2000), Settlements and damage caused by construction-induced vibrations. *Proceedings of the International Workshop: Wave 2000, Bochum, Germany, 13-15th December 2000*: 299-315
- Prakash S and Puri VK (2006), Foundations for vibrating machines. *Journal of Structural Engineering* 132(4): 1–39
- Reissner E (1936), Stationary and axially symmetrical vibrations of a Homogeneous Elastic Half-Space Caused by a Vibrating Mass, *Ing, Archiv, Band VII*, 281-396
- Sung TY (1953), Vibration in Semi-infinite Solid due to Periodic Surface Loading. *ASTM Special Technical Publication*, No 158, Symposium on Soil Dynamic, July, 35-64
- Terzaghi K (1955), Evaluation of Coefficients of Subgrade Reaction. *Géotechnique*, 5, 297-326
- Yang YB and Huang HH (1997), A parametric study of wave barriers for reduction of train induced vibrations. *International Journal of Numerical Methods in Engineering* (40): 3729-3747
- Yang YB, Huang HH and Chang DW (2003), Train-Induced Wave Propagation in Layered Soils Using Finite/Infinite element Simulation. *Soil Dynamics and Earthquake Engineering* (23): 263-278.